

Article

Fractional Sliding Mode Nonlinear Procedure for Robust Control of an Eutrophying Microalgae Photobioreactor

Abraham Efraim Rodríguez-Mata ^{1,*}, Ricardo Luna ², Jose Ricardo Pérez-Correa ³, Alejandro Gonzalez-Huitrón ¹, Rafael Castro-Linares ⁴ and Manuel A. Duarte-Mermoud ⁵

¹ Conacyt-Tecnológico Nacional de Mexico\Instituto Tecnológico de Culiacán, 80220 Culiacán Rosales, Mexico; victor.gonzalez@itculiacan.edu.mx

² Center for Research and Innovation (CRI), Viña Concha y Toro, 3550000 Penciahue, Chile; ricardo.luna@conchaytoro.cl

³ Chemical and Bioprocess Engineering Department, Pontificia Universidad Católica de Chile, Vicuña Mackenna 4860, Macul, Santiago, Chile; perez@ing.puc.cl

⁴ Department of Electrical Engineering, Center for Research and Advanced Studies of the National Polytechnic Institute (Cinvestav), 07360 Ciudad de Mexico, Mexico; rcastro@cinvestav.mx

⁵ Department of Electrical Engineering and Advanced Mining Technology Center (AMTC), University of Chile, Av. Tupper 2007, Santiago, Chile; mduartem@ing.uchile.cl

* Correspondence: aerodriguez@conacyt.mx or Arodriguez@itculiacan.edu.mx

Received: 16 December 2019; Accepted: 22 February 2020; Published: 26 February 2020

Abstract: This paper proposes a fractional-order sliding mode controller (FOSMC) for the robust control of a nonlinear process subjected to unknown parametric disturbances. The controller aims to ensure optimal growth in photobioreactors of native microalgae involved in eutrophication of the Sinaloa rivers in Mexico. The controller design is based on the Caputo fractional integral-order derivative and on the convergence properties of a sliding surface. For nonlinear systems, the proposed FOSMC guarantees convergence to the sliding surface even in the presence of model disturbances. The proposed controller is compared to an Internal Model Control (IMC) through numerical simulations.

Keywords: fractional-order control; sliding modes; stabilization; trajectory tracking; eutrophication control

1. Introduction

Water contamination due to human activity is increasing significantly, hampering our future development; hence, we should take immediate action and look for sustainable technologies to treat this vital resource. It is well known that some microorganisms are useful to remediate contaminated water; for example, microalgae are capable of eliminating organic nitrogen, the normal limiting substrate in wastewater [1]. Eutrophication refers to a significant increase in the concentration of nutrients of a given aquatic ecosystem due to human industrial activities. High nutrients availability leads to considerable proliferation of certain species of algae and higher aquatic plants. Proper control of microalgae growth either in photobioreactors or in the natural ambient (basins, rivers, and lakes) can reduce the concentration of pollutants generated by human activities. In Mexico, especially in the state of Sinaloa, eutrophication is critical. Hence, local authorities are looking for technologies, such as cultivation of microalgae in open photobioreactors, that can simultaneously aid the reduction of eutrophication and can be useful in producing biofuels [2].

The development of model-based automatic controllers for the robust operation of microalgae bioreactors will aid in the mitigation of water pollution as well as in the production of sustainable biofuels [3].

Mathematical models that describe the dynamics of algae growth and biofuel production in bioreactors present several complications such as

- strong nonlinearities; [3–5];
- high sensitivity to key variables (for example, temperature and pH variables) and to uncontrolled disturbances related to luminous intensity [6–8];
- growth rates highly sensitive to unmeasured disturbances [9,10]; and
- biomass growth generating space distribution and time-decay of incident light [11–13].

Some traditional control and estimation techniques, which are applied in biotechnological processes, usually do not cope well with unmeasured disturbances, and in some cases, it is difficult to find conditions that assure disturbance rejection [14–17]. Some previous contributions in the field guarantee a robust control [18,19]; however, these require perfect knowledge of all the states in the system. In practice, this is extremely difficult in photobioreactors due to the lack of reliable online measurements of metabolites and biomass concentrations [20]. On the other hand, Sliding Mode Control (SMC) is a well-known technique already successfully applied to photobioreactors [19,21]. However, this technique presents some theoretical and practical complications that hamper its application in industrial-scale bioreactors such as the monotonous switching feedback produced in the actuators, causing high-frequency flickering in the control action [21].

Given the above difficulties, it seems that fractional-order algorithms can be useful in the design of robust and scalable control systems for the culture of microalgae in photobioreactors [22]. Fractional control is an active research area, where many techniques have been developed to improve its performance and robustness as well as to combine it with other control methods [23]. Fractional control has proven to have many advantages over conventional and robust control techniques [24–27], such as more flexibility, the reduction of undesirable phenomena like chattering, and the generation of small continuous and derivative control signals. When using fractional-order sliding mode control (FOSMC), the fractional contribution significantly reduces the pitching effect of the system driven by the sliding modes [28–30].

Also, internal model control (IMC) has been used successfully to control nonlinear processes in batch mode. This controller has been designed by simulation and validated experimentally in alembic batch distillation [31,32]. The main advantages of this controller are the simple design when it is possible to identify a transfer function, the robustness to parameter model uncertainties, and the singular tuning parameter [33].

In this work, we design a nonlinear FOSMC system tolerant to internal model disturbances, based on the methodology proposed in Reference [30], for a microalgae photobioreactor that treats wastewater to reduce its nitrogen content. The FOSMC performance is evaluated through numerical simulations and compared to an IMC technique specifically designed for this process [18].

2. Process Modelling

A photobioreactor is a special type of bioreactor where photosensitive living organisms are cultivated [3]. Despite the complexity of the process dynamics of this system, it is possible to derive a treatable mathematical model that represents well the main features of the photobioreactor behavior [4]. Applying mass balances, the proposed model considers biomass concentration (represented by $x_1(t)$) and substrate concentration ($x_2(t)$) in the bioreactor [4]. The specific biomass growth rate mostly defines the bioreactor dynamics; hence, an accurate representation of this term is crucial (see, for example, Reference [3]). Our growth rate representation includes the substrate concentration and a complex global condition $\Sigma(\cdot)$, i.e., $\mu(x_2(t), \Sigma(\cdot)) = \mu(\cdot)$. This second component incorporates all those non-modelled effects that have a significant impact on the growth dynamics, such as sudden changes in pH, luminous intensity, metabolism, temperature, and substrate concentration gradients.

Biomass and substrate concentration dynamics are given by the corresponding mass balances in the fed-batch bioreactor:

$$\text{Accumulation} = \text{Inputs-Outputs} + \text{Generation-Consumption}.$$

Therefore,

$$\begin{aligned} \frac{d}{dt}(x_3(t)x_1(t)) &= x_3(t)\mu(\cdot)x_1(t), \\ \frac{d}{dt}(x_3(t)x_2(t)) &= -\alpha_1x_3(t)\mu(\cdot)x_1(t) + \alpha_2u(t), \\ \frac{d}{dt}x_3(t) &= u(t), \end{aligned} \quad (1)$$

where $x_3(t)$ is the bioreactor volume, α_1 is the substrate/biomass yield coefficient, α_2 is the substrate concentration in the inlet stream, and $u(t)$ is the control variable which in this case is the inlet stream flow-rate. Usually, the volume varies until a desirable steady state is reached (fed-batch operation), after which the bioreactor is operated in continuous mode (constant volume and equal inlet and outlet flow-rates). In this paper, we are only concerned with the fed-batch stage. Equation (1) can be written as follows:

$$\begin{aligned} \frac{dx_3}{dt}x_1(t) + \frac{dx_1(t)}{dt}x_3(t) &= x_3(t)\mu(\cdot)x_1(t), \\ \frac{dx_3}{dt}x_2(t) + \frac{dx_2(t)}{dt}x_3(t) &= -\alpha_1x_3(t)\mu(\cdot)x_1(t) + \alpha_2u(t), \\ \frac{dx_3}{dt} &= u(t), \end{aligned} \quad (2)$$

or, equivalently,

$$\begin{aligned} \dot{x}_1 &= \mu(\cdot)x_1(t) - \frac{u(t)}{x_3(t)}x_1(t), \\ \dot{x}_2 &= -\alpha_1\mu(\cdot)x_1(t) + \frac{u(t)}{x_3(t)}(\alpha_2 - x_2(t)), \\ \dot{x}_3 &= u(t). \end{aligned} \quad (3)$$

An unknown additive disturbance function $\Sigma(\cdot) = f(pH, T, P, \nabla x_2(t), I_{av}(t))$ is assumed to be present in the dynamics of x_1 and x_2 , where $pH = pH(t)$, $T = T(t)$ is the temperature, $P = P(t)$ is the pressure, $\nabla x_2(t)$ is the substrate concentration gradient, and $\nabla I_{av}(t)$ is the average luminous intensity. We consider the following assumption for function $\Sigma(\cdot)$.

Assumption 1. The disturbance function $\Sigma(\cdot)$ is bounded by a strictly nonnegative smooth function $\delta(t)$, which is bounded by a positive real number δ_{max} :

$$|\Sigma(\cdot)| \leq \delta(t) \leq \delta_{max}. \quad (4)$$

In addition, we consider that the effect of substrate concentration on biomass growth rate is well represented by the Monod model. This is one of the most used biomass growth kinetic models, since it is a good compromise between accuracy and simplicity. Moreover, this kinetic model will

allow us to develop analytically appropriate feedback control laws that will compensate the effects of non-modeled disturbances. More precisely, we consider the following model:

$$\mu_m = \frac{a_1 x_2(t)}{x_2(t) + a_2}, \tag{5}$$

with $\mu_m = \mu_{monod}(x_2(t))$. Thus, it is proposed in this paper that the dynamic complex denoted by $\mu(\cdot)$ is the arithmetic sum of two terms, the Monod kinetics, and the bounded non-modeled disturbance function:

$$\mu(\cdot) = \mu_m + \Sigma(\cdot). \tag{6}$$

Assumption 2. Most dynamic bioreactor models satisfy the bounding condition over the expected disturbances in the growth rate, since the following triangle inequality is satisfied: $|\mu(\cdot)| \leq |\mu_m| + |\Sigma(\cdot)| \rightarrow |\Sigma(\cdot)| < |\mu(\cdot)|$. Therefore, $\delta_{max} < |\mu(\cdot)|$. The maximum disturbance should be less than the net biochemical reaction rate, thus ensuring that it will be rejected and that, consequently, the system will be brought to the simplified reference dynamics given by Monod.

For example, toxic and inhibitory agents, such as excess average light intensity in microalgae cultivation [2], reduce the growth rate. This effect can be modelled as an unknown function $\Sigma(\cdot)$ that is subtracted from the optimal growth rate given by the Monod expression, μ_m (see Figure 1).

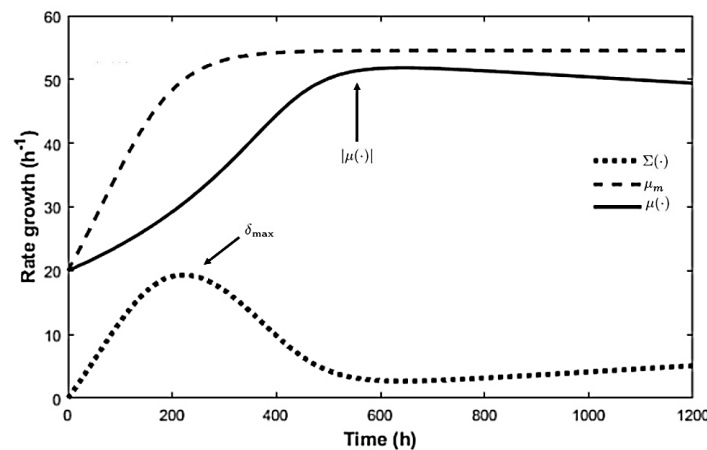


Figure 1. Dynamics obtained using $\mu(\cdot) = \mu_m + \Sigma(t)$; $\mu(\cdot) = \frac{a_1 x_2(t)}{a_2 + x_2(t) + a_3 x_2^2}$, and $\mu_m = \frac{a_1 x_2(t)}{x_2(t) + a_2}$, with $a_1 = 0.026h^{-1}$, $a_2 = 9.82 \text{ mg/L}$, and $a_3 = 0.0254 \text{ lux.L/mg}$; see Reference [1]. a_3 is a constant that depends on the minimum inhibitory amount of light, I_{max} .

Replacing Equation (6) into Equation (3) yields the main mathematical model used in this paper:

$$\begin{aligned} \dot{x}_1 &= \mu_m x_1(t) - \left(\frac{u(t)}{x_3(t)} + \Sigma(t) \right) x_1(t), \\ \dot{x}_2 &= -\alpha_1 \mu_m x_1(t) + \frac{u(t)}{x_3(t)} (\alpha_2 - x_2(t)) - \alpha_1 \Sigma(t) x_1(t), \\ \dot{x}_3 &= u(t), \\ \mu_m &= \frac{a_1 x_2(t)}{a_2 + x_2(t)}. \end{aligned} \tag{7}$$

Since the disturbance function appears in a bilinear relationship with one of the states of the system, the effects of the unknown dynamics $\Sigma(\cdot)$ can be compensated with an appropriate robust disturbance rejection control technique.

The optimal steady state is computed based on the Monod kinetics [9,34]; however, disturbance terms such as $\Sigma(\cdot)$ drive the system to unwanted suboptimal steady states. This is a commonly experienced limitation in the control of photobioreactors. In addition, the optimal transition from batch to continuous mode operation is challenging. In this paper, we propose a control method which is robust against the disturbance term $\Sigma(\cdot)$, which is present in the fed-batch stage of the operation of photobioreactors. We also expect that the control algorithm will be equally effective in the continuous mode operation stage; hence, the reference model of the control system is the nominal one associated with the continuous mode operation of the photobioreactor (without disturbances) while the fed-batch disturbed model will be the plant to be stabilized.

3. A Fractiona-Order Sliding Mode Controller (FOSMC)

Fractional calculus is the extension of classical calculus to derivation and integration operations using non-integer orders. In the time domain, fractional (non-integer) derivatives and integrals are defined by the convolution operation. Hence, they are especially suited to representing memory phenomena, with several applications in science and engineering [35]. In this paper, a fractional-order sliding mode controller (FOSMC) is proposed in order to track a predefined operating path of a photobioreactor (eutrifying microalgae photobioreactor). The Riemann–Liouville and Caputo definitions of fractional operators are the most used. In this work, the Caputo definition is used. According to Reference [36], the Caputo fractional derivative of order β of function $\phi(t)$ on the half-positive real axis is defined as

$$D^\beta \phi(t) = \frac{1}{\Gamma(n - \beta)} \int_0^t \frac{\phi^{(n)}(\tau)}{(t - \tau)^{\beta+n-1}} d\tau, \tag{8}$$

where $\phi(t)$ is a function assumed to be sufficiently smooth and locally integrable; Γ is the so-called gamma function defined as $\Gamma(n) = \int_0^\infty t^{n-1} e^{-t} dt$; and $n - 1 < \beta < n$, with n being an integer. This Caputo definition is used the most in engineering applications since this definition incorporates initial conditions for $\phi(t)$ and its integer-order derivatives; this is initial conditions that are physically appealing in the traditional way. Notice that $\phi^{(n)}(t)$ stands for the integer derivative of order n of function $\phi(t)$ in Equation (8). Also, to simplify the notation, we will denote the Caputo fractional derivative of order β of function $\phi(t)$, $D^\beta \phi(t)$, as $\phi^{(\beta)}$. In addition, the fractional integral of order β of function $\phi(t)$ on the half-positive real axis is defined, also in accordance with [36], as

$$I^\beta \phi(t) = \frac{1}{\Gamma(\beta)} \int_0^t \frac{\phi(\tau)}{(t - \tau)^{1-\beta}} d\tau, \tag{9}$$

where β is the fractional order defined above. It is important to notice that the notation $D^{-\beta} \phi(t)$ is used as well as to denote the fractional integral of order β of function $\phi(t)$, more precisely $D^{-\beta} \phi(t) \equiv I^\beta \phi(t)$. The definitions of fractional derivative and fractional integral, as stated above, cannot be used in practice; thus, numeric methods such as the one based on the Grünwald–Letnikov approach are commonly used [37].

We consider the following first-order nonlinear perturbed system:

$$\dot{x}(t) = f(x) + g(x)u(t) + \delta(x), \tag{10}$$

where $f(x)$ and $g(x)$ are bounded, smooth, and locally integrable functions; $u(t)$ is a scalar input variable; and $\delta(x) \in \mathbb{R}$ is a disturbance term that satisfies the bound in Equation (4) in Assumption 1.

To design a reference tracking controller, the reference signal $x(t)_{ref} = x_r$ is proposed together with the tracking error:

$$e = x_r - x. \quad (11)$$

Based on the sliding mode control methodology [38], the following switching function s is then proposed:

$$s(t) = e(t) + k_1 \int_0^t e(\tau) d\tau, \quad (12)$$

where k_1 is a nonzero positive real parameter. The switching function in Equation (12) defines the sliding surface

$$s = 0 = e(t) + k_1 \int_0^t e(\tau) d\tau, \quad (13)$$

for which k_1 is selected in such a way that the corresponding first-order differential equation $0 = \dot{e} + k_1 e$ has a solution that exponentially converges to zero; as a consequence, x converges to x_r exponentially when the system dynamics is constrained to the sliding surface in Equation (13).

The nominal system associated to the perturbed system in Equation (10) with $\delta(x) = 0$ for all x is given by

$$\dot{x}(t) = f(x) + g(x)u(t). \quad (14)$$

In order to attract the dynamics of the system in Equation (10) to the sliding surface in Equation (13) and based on the strategy proposed in Reference [39], the first-order time derivative of s is set to be the following (see, for example, Reference [38])

$$\dot{s} = -k_2 I^\beta \text{sgn}(s) - k_3 s, \quad (15)$$

with k_2 and k_3 being nonzero positive real parameters and $\text{sgn}(\cdot)$ being the signum function. On the other hand, from the switching function in Equation (12) and the nominal system in Equation (14), \dot{s} is given by

$$\dot{s} = \dot{x}_r - f(x) - g(x)u + k_1 e. \quad (16)$$

Combining Equations (15) and (16) leads to the following fractional-order sliding mode controller:

$$u = -\frac{1}{g(x)}(f(x) + \eta(x, x_r)), \quad (17)$$

with

$$\eta(x, x_r) = -k_2 I^\beta \text{sgn}(s) - k_3 s - \dot{x}_r - k_1 e.$$

A sufficient condition that assures the attraction of the perturbed nonlinear system in Equation (10) to the sliding surface in Equation (13) can be given. This is stated in the following theorem.

Theorem 1. *Let us consider the perturbed first-order nonlinear system in Equation (10) with a bounded disturbance $\delta(x)$ that satisfies Equation (4). That is, Assumption 1 holds. If the parameter k_2 and the bound δ_{max} satisfy*

$$k_2 \left| I^\beta \text{sgn}(s) \right| > \delta_{max}, \quad (18)$$

then the fractional order sliding mode controller in Equation (17) assures the attractiveness of the perturbed system to the sliding surface $s = 0$.

Proof. Consider the Lyapunov function candidate

$$V = \frac{1}{2}s^2, \quad (19)$$

which is positive definite. The time derivative of V along the trajectories of the perturbed system dynamics together with the fractional-order controller in Equation (17) takes the following form:

$$\dot{V} = s\dot{s} = s(\dot{x}_r - \dot{x} + k_1e) = -k_2(I^\beta \text{sgn}(s))s - k_3s^2 - s\delta. \quad (20)$$

Since $s = |s|\text{sgn}(s)$ and $\text{sgn}(D^{-\beta}\text{sgn}(s)) = \text{sgn}(s)$, for $0 < \beta < 1$ [39], \dot{V} can be written as

$$\dot{V} = k_2 |s| \left| I^\beta \text{sgn}(s) \right| - k_3s^2 - s\delta. \quad (21)$$

Now majoring Equation (21) and using the bound δ_{max} in Assumption 1, one obtains

$$\dot{V} \leq -k_3s^2 - |s| (k_2 \left| I^\beta \text{sgn}(s) \right| - \delta_{max}). \quad (22)$$

Notice that the term k_3s^2 is always positive. Thus, if condition (18) is satisfied, $\dot{V} < 0$ and the convergence to the surface $s = 0$ is assured. \square

Remark 1. The main idea of the fractional-order sliding mode controller design proposed here is to define a switching function (Equation (12)), together with its first-order derivative (Equation (15)), such that, when the disturbance appears, s is different from zero and, at that time, the discontinuous control term becomes active and rejects the disturbance.

Remark 2. From the proof of Theorem 1, it can be noticed that the following sufficient condition allows us to obtain the attraction of the perturbed nonlinear system to the sliding surface $s = 0$.

$$k_2 \left| I^\beta \text{sgn}(s) \right| + k_3 |s| > \delta_{max}, \quad (23)$$

In fact, the condition in Equation (23) shows that a stronger attraction to $s = 0$ is achieved and that the attraction is higher for any value of s with $k_3 \neq 0$. However, the condition in Equation (23) is more restrictive since it requires the knowledge of $|s|$ at every time t .

Application to a Photobioreactor

The simplified model of the photobioreactor in Equation (3) represents its dynamics well if disturbances such as $I(t)$, $pH(t)$, etc. are kept regulated. However, these and other disturbances vary unexpectedly in experimental photobioreactors, making its control very difficult. Even if the expanded model in Equation (7) can better represent the complex dynamic behavior of the experimental system, the disturbance function is a priori unknown. Consequently, this model cannot be used to design a robust controller. Moreover, developing a control law using this expanded model is difficult. Instead, in this paper, we use a simplified model that only considers the dynamics of the measured variable (biomass concentration) to design a FOSMC to achieve robust control of the photobioreactor. This approach has been successfully used before for robust bioreactor control [9,40], assuring asymptotic stability of the main state, while the rest of the system is kept bounded. In this paper, we design a FOSMC to achieve robust tracking of $x_1(t)$ to a reference signal while keeping the substrate $x_2(t)$ and the volume $x_3(t)$ bounded.

The reduced model used to design the control is given by

$$\begin{aligned} \dot{x}_1 &= \mu_m x_1 - \frac{x_1}{x_3} u + \Sigma x_1, \\ \mu_m &= \frac{a_1 x_2}{a_2 + x_2}, \end{aligned} \tag{24}$$

where $x_1(t) = x_1 \geq 0$, $x_2(t) = x_2 \geq 0$, $x_3(t) = x_3 \geq 0$, $u(t) = u \geq 0$, and $\Sigma(t) = \Sigma$. Thus, when considering an optimal reference biomass dynamics $x_{1,r}$, the following robust FOSMC is proposed:

$$\begin{aligned} u &= -(\mu_m x_1 + \eta(x_1, x_{1,r})) \frac{x_3}{x_1}, \\ \eta(x_1, x_{1,r}) &= -k_2 I^\beta \text{sgn}(s) - k_3 s - \dot{x}_{1,r} - k_1 e, \\ e &= x_{1,r} - x, \\ s &= e + k_1 \int_0^t e(\tau) d\tau. \end{aligned} \tag{25}$$

The structure of the designed controller is shown in Figure 2. The numerical simulations carried out when using this fractional-order controller are given in Section 5.

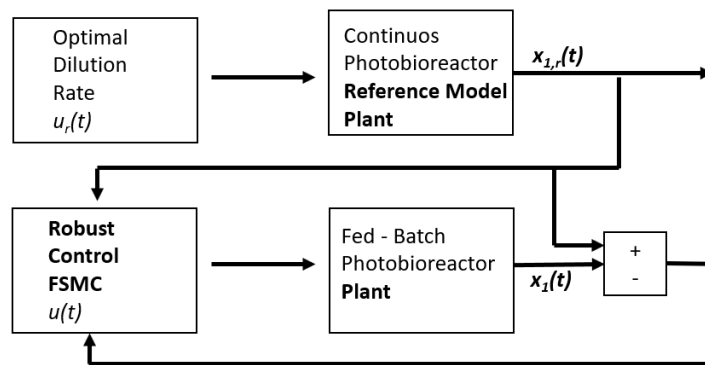


Figure 2. Conceptual diagram of the photobioreactor control simulation.

4. Internal Model Control (IMC)

The IMC is based on an ideal control system that would force the process output to track its setpoint suppressing all disturbances. The IMC control algorithm corresponds to the inverse of the process model [33]. For a first-order plus delay time (FOPDT) transfer function model, the IMC is given by the following:

$$C_{IMC}(s) = \frac{\tau \cdot s + 1}{k \cdot (\varepsilon \cdot s + 1)^\alpha}, \tag{26}$$

where τ is the process time constant, k is the process gain, ε is the filter time constant (tuning parameter of IMC), and α is the relative order of the inverse of the process model (in this case, $\alpha = 1$). The transfer function was obtained using the process reaction curve to a step change in the manipulated variable around the optimal inlet stream flow-rate (0.018 L/h) in continuous mode operation [1]. Table 1 shows the fitted parameters of the process model.

Table 1. Parameters of the Internal Model Control (IMC) applied to the photosynthetic plant.

Parameter	Value
k	−30,119
θ	1
τ	60.5

5. Numerical Simulation

To assess the effectiveness of the proposed FOSMC controller, a numerical simulation of the controlled photobioreactor was carried out in Matlab/Simulink using the FOMCON toolbox [37]. The simulation considered the transition from batch operation to continuous operation. In this transition, where the photobioreactor operates in fed-batch mode, the controller should ensure that the biomass concentration follows a predefined path as close as possible despite unmeasured disturbances. This means that the system in Equation (7) should follow the dynamics of the reference model until the maximum volume, $x_3(t)$, is reached. The reference model is given by the following:

$$\begin{aligned}
 \dot{x}_{1r} &= \mu_m x_1(t) - u(t)x_1(t), \\
 \dot{x}_{2r} &= -\alpha_1 \mu_m x_{1r}(t) + u(t)(\alpha_2 - x_{2r}(t)), \\
 \mu_{mr} &= \frac{a_{1,nom} x_{2r}(t)}{a_{2,nom} + x_{2r}(t)},
 \end{aligned} \tag{27}$$

where $a_{1,nom}$ and $a_{2,nom}$ are the nominal model parameters (used in the design of the controller). The non-modelled disturbance function Σ in Equation (7) represents in our case model parameter changes due to unmeasured variations in light incidence, pH, and substrate concentration gradients. We consider that all these disturbances impact only the maximum specific growth rate as an additive term, i.e., $a_1(t) = a_{1,nom} + \delta(t)$. It is assumed that this additive term suffers step changes at arbitrary times. Therefore, the Σ function has the following structure:

$$\begin{aligned}
 \dot{x}_1 &= \mu_m x_1 - \frac{x_1}{x_3} u + \Sigma x_1, \\
 \mu_m &= \frac{a_{1,nom} x_2}{a_2 + x_2}, \\
 \Sigma &= \frac{\delta(t) x_2}{a_2 + x_2}.
 \end{aligned} \tag{28}$$

Since the maximum norm $\delta(t)$ and the a_2 constant are positive, the maximum Σ disturbance value will always be limited by the measurable state at the output, so it is possible to expand the FOSMC shown in Equation (25) for the reduced system in Equation (28), such that $a_2, \delta(t) \neq 0 \rightarrow \|\Sigma\| \leq \|x_2\| \leq \alpha_1^{-1} \|x_1\|$,

Therefore, the trajectory tracking error is $e = x_{r1} - x_1$. The numerical simulation parameters are given in the following Table 2.

Table 2. Simulation parameters of the reference plant and the simulated fed-batch plant, where u_r is an optimal open loop feed flow for the continuous photobioreactor model.

Parameters	Plant	Reference plant	Units
$a_{1,nom}$	0.027	0.027	h^{-1}
a_2	9.25	9.25	mg/L
α_1	3.45	3.45	- - -
α_2	205	205	mg/L
$x_1(0)$	600	540	mg/L
$x_2(0)$	80	60	mg/L
$x_3(0)$	0.001	NA	L
$x_{r1}(0)$	NA	540	mg/L
$x_{r1}(0)$	NA	60	mg/L
$x_{3,max}$	3	3	L
u_r	NA	0.001	L/h

A robust FOSMC is proposed for the system in Equation (28) as follows:

$$\begin{aligned}
 u &= -(\mu_m x_1 + \eta(\cdot)) \frac{x_3}{x_1}, \\
 \eta(\cdot) &= -k_2 I^\beta \text{sgn}(s) - k_3 s - \mu_m x_{r1} - x_{r1} u_r - k_1 e \\
 s &= e + k_1 \int_0^t e(\tau) d\tau, \\
 \mu_m &= \frac{a_{1,nom} x_2}{a_2 + x_2}.
 \end{aligned}
 \tag{29}$$

The process is simulated in Matlab/Simulink with a variable step Dormand–Prince numerical method. The simulation experiment considers 500 h of cultivation of the microalgae *Spirulina Maxima*, according to real-time experiments taken from the literature, see to Table 3.

Table 3. Parameters of the FOSMC controller applied to the photosynthetic plant.

Parameters	Value
k_1	5
k_2	0.12
k_3	0.12
$a_{1,nom}$	0.027
a_2	25
β	0.3, 0.6, 0.9, and 1
$\delta(t)$	see Figure 3

The complete nonlinear dynamics of the photobioreactor in Equation (7) is simulated using a robust FOSMC control law (Equation (29)) in the presence of $\delta(t)$ disturbances on parameter a_1 (see Figure 3).

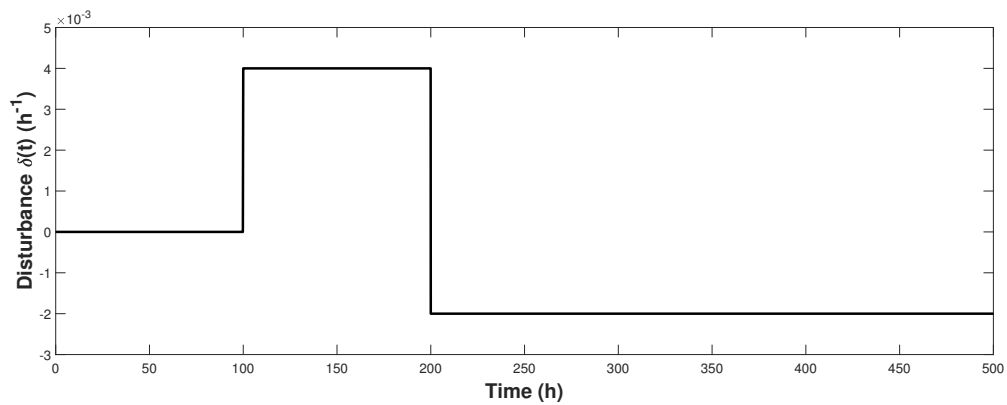


Figure 3. Dynamics of the disturbance $\delta(t)$ assessed in the numerical simulation experiment.

The FOSMC in Equation (29) is much better than optimal open-loop operation in the presence of disturbances. Basically the same closed-loop dynamics of the biomass (Figure 4), substrate (Figure 5), and control (Figure 6) were obtained for 5 different values of the integral fractional order (β factors). However, different sliding surface dynamics were obtained (see Figure 7). β values are key to assuring convergence of the surface. With $\beta = 0.1$, the sliding surface does not converge to zero (Figure 7). In addition, the fractional-order value affects the speed of convergence of the sliding surface. Values higher than or equal to 0.9 provide high convergence rates, although with oscillations; $\beta = 0.6$ seems to be a good compromise giving a smooth and fast convergence.

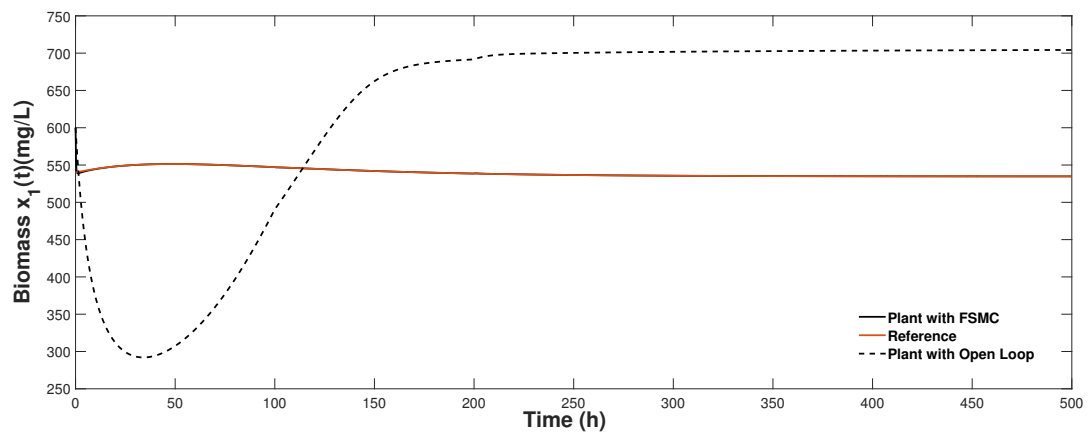


Figure 4. Biomass dynamics under FOSMC control compared to optimal open-loop operation.

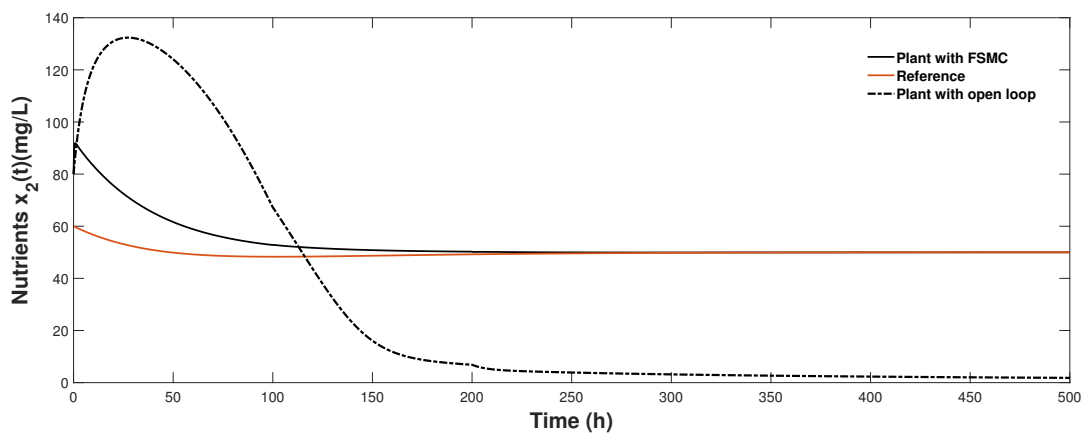


Figure 5. Substrate dynamics under FOSMC control compared to optimal open-loop operation.

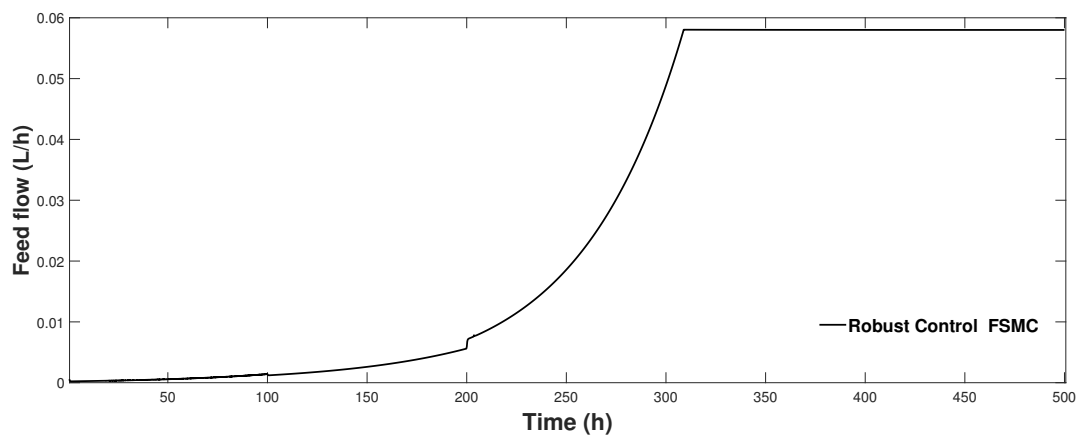


Figure 6. Control variable dynamics (feed flow, $u(t)$ of Equation (29)).

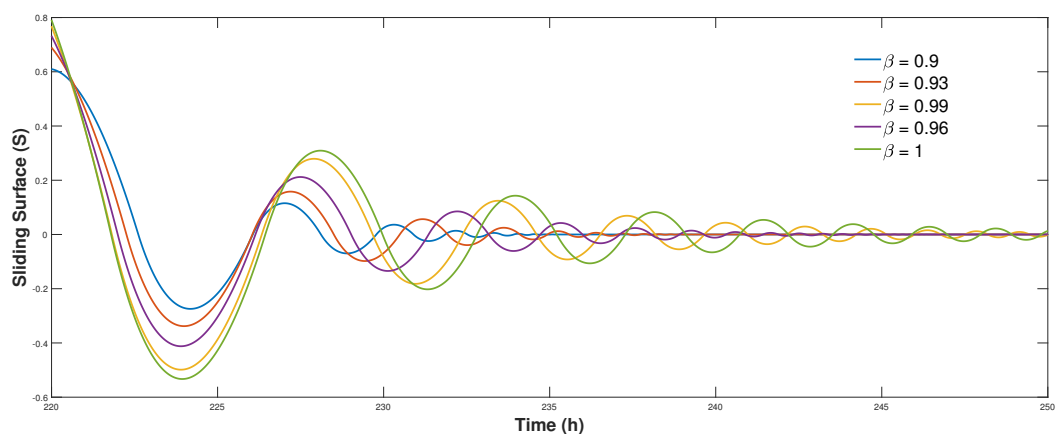


Figure 7. Dynamics of the sliding surface $\dot{s} = \dot{e} + k_1e$ applying different values of fractional-order integration.

5.1. Effect of β Value on Performance

To analyze more precisely how β values affect control performance, additional simulations were carried out with $\beta = 0.9, 0.93, 0.96, 0.99, 1$. Performance was assessed using the Integral time absolute error (ITAE).

Figure 8 shows that, when β is closer to 1, performance worsens. Hence, fractional-order control not only eliminates the chattering problem and improves convergence to the sliding surface but also reduces tracking error.

5.2. Comparison of FOSMC with Internal Model Control (IMC).

Here, the same simulation parameters as above and $\beta = 0.9$ were used. The FOSMC has been compared with an IMC in the simulation of the photobioreactor subjected to the same model parameter disturbances described above. The IMC is a controller that has been thoroughly studied in the literature. It has proven to be robust to certain types of disturbances when applied to bioprocess control. The FOSMC used the mean integration order constant 0.5 and the IMC used the filter time constant $\varepsilon = 0.1$ h (tuned by trial and error).

Figures 8 and 9 show that the FOSMC is superior to the IMC when model parameters are subjected to disturbances. Even though model parameter ($a_1(t)$) changes at times 100 and 200 h, deviations from the biomass optimal path started to appear at time 200 h, reaching a maximum deviation at time 340 h. In turn, the FMSC perfectly tracked the biomass optimal path since it kept the controlled system on the sliding surface (see to Figures 10 and 11). Several control quality indices were computed to compare both controllers: the integral of the time-weighted absolute error (ITAE), the integral of the absolute error (IAE), the integral of the square error (ISE), the integral of the square control signal input (ISI), and the integral of the absolute control signal input (IAI).

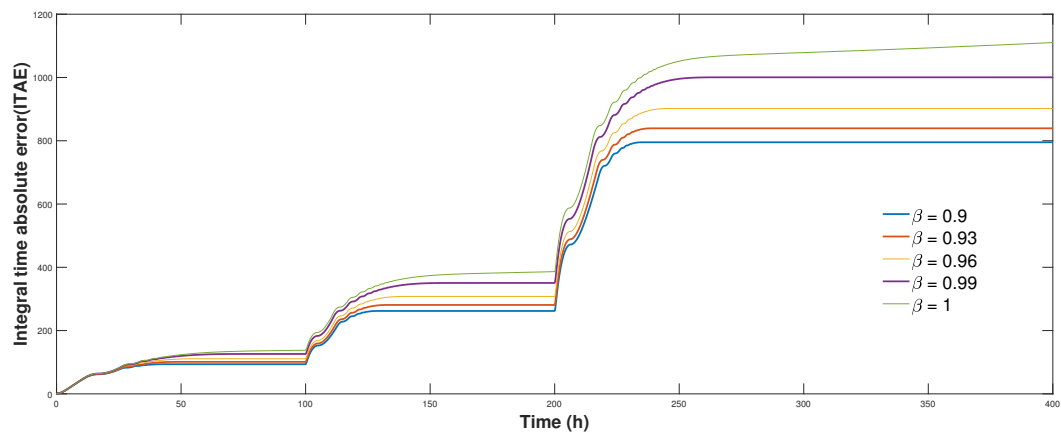


Figure 8. Effect of β value on ITAE evolution.

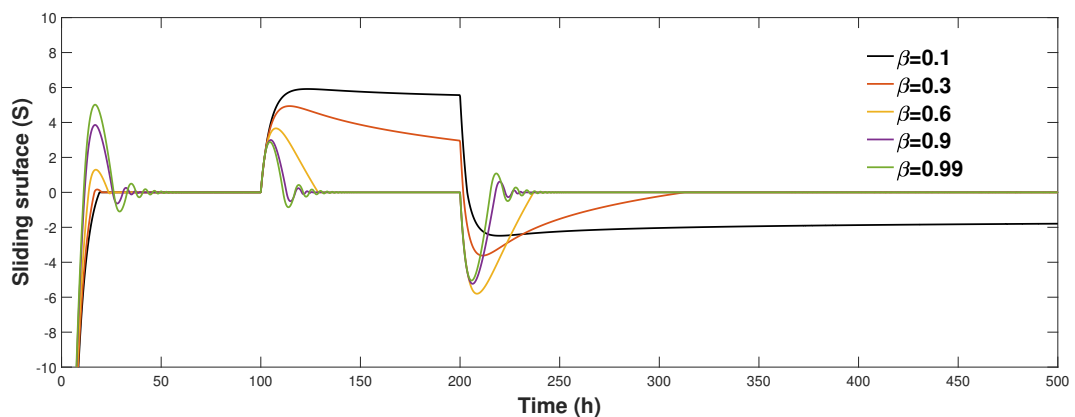


Figure 9. Dynamics of the sliding surface $\dot{s} = \dot{e} + k_1e$ applying different values of fractional-order integration.

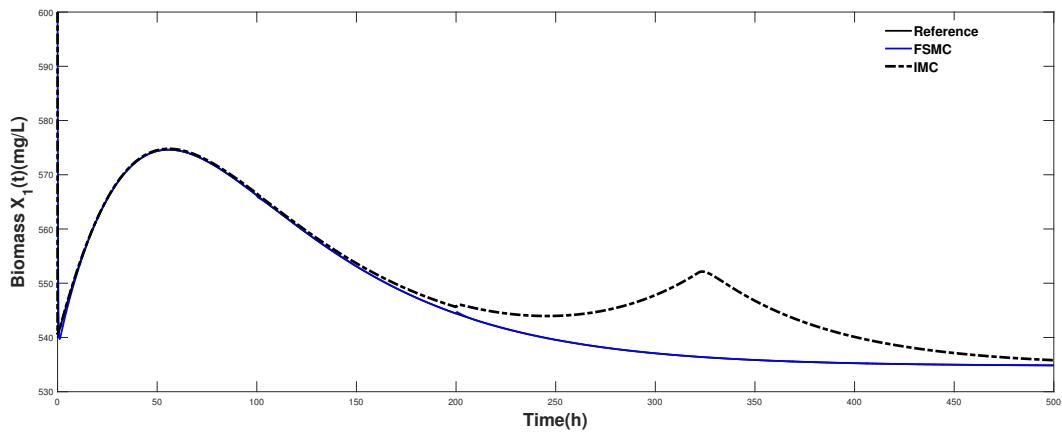


Figure 10. Numerical comparison between the IMC and the FMSC in the presence of parametric disturbances in a photobioreactor.

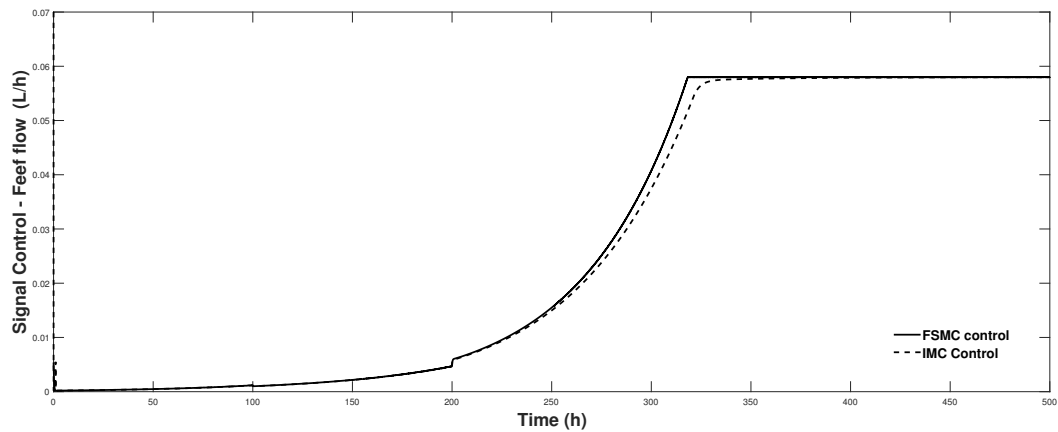


Figure 11. Evolution of the manipulated variables of the two controllers.

These indices also show that the FOSMC performed much better than the IMC. Both control signals are equally smooth since indices ISI and IAI are practically the same, as shown in Table 4. Hence, highly nonlinear and complex systems like photobioreactors require robust nonlinear control techniques, such as the proposed FOSMC, to achieve acceptable performance.

Table 4. Integral criteria for the evaluation of the performance of the controllers at 500 hr of the process

Parameter	FOSMC	IMC
ITAE	740.6	6.04e5
IAE	25	1863
ISE	347	1.59e4
ISI	0.6981	0.6801
IAI	13.53	13.3

6. Conclusions

A fractional-order sliding mode controller (FOSMC) has been proposed for tracking a specified trajectory in a photobioreactor. This trajectory optimally transferred the bioreactor from batch to continuous mode of operation. As far as the authors are aware, this is the first time that an FOSMC algorithm is designed to control a photobioreactor. The FOSMC can assure that the disturbed system

will converge to a sliding surface despite model parameter disturbances. In addition, it was observed in simulations that the integration fractional order affects this convergence rate. The proposed algorithm could also be a good choice to control other highly nonlinear bioreactors.

Author Contributions: Conceptualization, A.E.R.-M., R.L., J.R.P.-C., R.C.-L.; Writing—review and editing, A.E.R.-M., R.L., J.R.P.-C., R.C.-L.; Methodology, A.E.R.-M., R.L., J.R.P.-C., R.C.-L.; Project administration, M.A.D.-M.; Software, A.G.-H. All authors have read and agreed to the published version of the manuscript.

Acknowledgments: This work has been supported by CONICYT-Chile (ANID-Chile), under the grants FONDECYT 1150488 "Fractional Error Models in Adaptive Control and Applications", FONDECYT 1190959 "Development of Fractional Order Tools for Stability, Estimation and Control of Systems and Applications" and CONICYT Project AFB180004.

Conflicts of Interest: The authors declare no conflict of interest.

References

1. Dominguez-Bocanegra, A.R.; Torres-Muñoz, J.A.; Carmona, R.; Aguilar-Lopez, R. Theoretical-practical study on the removal of contaminants in Los Remedios River (State of Mexico). *Ingeniería Hidráulica en México* **2009**, *24*, 81–91.
2. Gomez-Villa, H.; Voltolina, D.; Nieves, M.; Pina, P. Biomass production and nutrient budget in outdoor cultures of *Scenedesmus obliquus*(Chlorophyceae) in artificial wastewater, under the winter and summer conditions of Mazatlan, Sinaloa, Mexico. *Vie et milieu* **2005**, *55*, 121–126.
3. Bernard, O. Hurdles and challenges for modelling and control of microalgae for CO₂ mitigation and biofuel production. *J. Process Contr.* **2011**, *21*, 1378–1389. [[CrossRef](#)]
4. Rodríguez-Mata, A.; Flores-Colunga, G.; Rangel-Peraza, J.; Lizardi-Jiménez, M.; Amabilis-Sosa, L. Estimation of states in photosynthetic systems via chained observers: design for a tertiary wastewater treatment by using *Spirulina maxima* on photobioreactor. *Rev. Mex. Ing. Quím.* **2019**, *18*, 273–287. [[CrossRef](#)]
5. Garzón-Castro, C.L.; Delgado-Aguilera, E.; Cortés-Romero, J.A.; Tello, E.; Mazzanti, G. Performance of an active disturbance rejection control on a simulated continuous microalgae photobioreactor. *Comput. Chem. Eng.* **2018**, *117*, 129–144. [[CrossRef](#)]
6. Keesman, K.J.; Stigter, J.D. Optimal parametric sensitivity control for the estimation of kinetic parameters in bioreactors. *Math. Biosci.* **2002**, *179*, 95–111. [[CrossRef](#)]
7. Fitzpatrick, J.J.; Gloanec, F.; Michel, E.; Blondy, J.; Lauzeral, A. Application of Mathematical Modelling to Reducing and Minimising Energy Requirement for Oxygen Transfer in Batch Stirred Tank Bioreactors. *Chemengineering* **2019**, *3*, 14. [[CrossRef](#)]
8. Banerjee, S.; Ramaswamy, S. Dynamic process model and economic analysis of microalgae cultivation in flat panel photobioreactors. *Algal Res.* **2019**, *39*, 101445. [[CrossRef](#)]
9. Mata, A.E.R.; Munoz, J.T.; Correa, J.R.P.; Bocanegra, A.R.D.; Luna, R.; Flores, G. Robust State Estimation in Presence of Parametric Uncertainty by NL-PI observers. An Application to Continuous Microbial Cultures. *Lat. Am. Trans. IEEE* **2016**, *14*, 1199–1205.
10. Liu, W.C.; Inwood, S.; Gong, T.; Sharma, A.; Yu, L.Y.; Zhu, P. Fed-batch high-cell-density fermentation strategies for *Pichia pastoris* growth and production. *Crit. Rev. Biotechnol.* **2019**, *39*, 258–271. [[CrossRef](#)] [[PubMed](#)]
11. Nwoba, E.G.; Parlevliet, D.A.; Laird, D.W.; Alameh, K.; Moheimani, N.R. Light management technologies for increasing algal photobioreactor efficiency. *Algal Res.* **2019**, *39*, 101433. [[CrossRef](#)]
12. Yen, H.W.; Hu, I.C.; Chen, C.Y.; Nagarajan, D.; Chang, J.S. Design of photobioreactors for algal cultivation. In *Biofuels from Algae*; Elsevier: New York, NY, USA, 2019; pp. 225–256.
13. Pruvost, J. Cultivation of algae in photobioreactors for biodiesel production. In *Biofuels: Alternative Feedstocks and Conversion Processes for the Production of Liquid and Gaseous Biofuels*; Elsevier: New York, NY, USA, 2019; pp. 629–659.
14. Gustavsson, R. *Development of Soft Sensors for Monitoring and Control of Bioprocesses*; Linköping University Electronic Press: Linköping, Sweden, 2018; Volume 954.
15. Parada, P.A.L.; Pettersen, E.; Bar, N. Bioreactor Scaling Enhances Feedback Control Of Concentration, Rates, and Yields. *IFAC-PapersOnLine* **2019**, *52*, 237–242. [[CrossRef](#)]

16. Ramaswamy, S.; Cutright, T.; Qammar, H. Control of a continuous bioreactor using model predictive control. *Process Biochem.* **2005**, *40*, 2763–2770. [[CrossRef](#)]
17. Nguyen, D.; Gadhamshetty, V.; Nitayavardhana, S.; Khanal, S.K. Automatic process control in anaerobic digestion technology: A critical review. *Bioresour. Technol.* **2015**, *193*, 513–522. [[CrossRef](#)] [[PubMed](#)]
18. Rodriguez-Mata, A.; Torres-Muñoz, J.; Domínguez-Bocanegra, A.; Flores, G.; Rangel-Peraza, G. Nonlinear robust control for a photobioreactor in presence of parametric disturbances. *Rev. Mex. Ing. Quim.* **2016**, *15*, 985–993.
19. Coutinho, D.; Vargas, A.; Feudjio, C.; Benavides, M.; Wouwer, A.V. A robust approach to the design of super-twisting observers—application to monitoring microalgae cultures in photo-bioreactors. *Comput. Chem. Eng.* **2019**, *121*, 46–56. [[CrossRef](#)]
20. Farza, M.; Rodriguez-Mata, A.; Robles-Magdaleno, J.; M'Saad, M. A new filtered high gain observer design for the estimation of the components concentrations in a photobioreactor in microalgae culture. *IFAC-PapersOnLine* **2019**, *52*, 904–909. [[CrossRef](#)]
21. de Andrade, G.A.; Pagano, D.J.; Guzmán, J.L.; Berenguel, M.; Fernández, I.; Ación, F.G. Distributed sliding mode control of pH in tubular photobioreactors. *IEEE Trans. Contr. Syst. Tech.* **2015**, *24*, 1160–1173. [[CrossRef](#)]
22. Yadav, V.K.; Das, S.; Bhadauria, B.S.; Singh, A.K.; Srivastava, M. Stability analysis, chaos control of a fractional order chaotic chemical reactor system and its function projective synchronization with parametric uncertainties. *Chin. J. Phys.* **2017**, *55*, 594–605. [[CrossRef](#)]
23. Duarte-Mermoud, M.A.; Aguila-Camacho, N.; Linares, R.C. Position control of the Thomson's ring system using fractional operators. *Int. J. Circ. Syst. Signal Process.* **2015**, *9*, 344–352.
24. Aguila-Camacho, N.; Duarte-Mermoud, M.A.; Gallegos, J.A. Lyapunov functions for fractional order systems. *Comm. Nonlinear Sci. Numer. Simulat.* **2014**, *19*, 2951–2957. [[CrossRef](#)]
25. Zamani, M.; Karimi-Ghartemani, M.; Sadati, N.; Parniani, M. Design of a fractional order PID controller for an AVR using particle swarm optimization. *Contr. Eng. Pract.* **2009**, *17*, 1380–1387. [[CrossRef](#)]
26. Maiti, D.; Biswas, S.; Konar, A. Design of a fractional order PID controller using particle swarm optimization technique. *arXiv* **2008**, arXiv:0810.3776. Available online: <https://arxiv.org/ftp/arxiv/papers/0810/0810.3776.pdf> (accessed on 22 December 2019).
27. von Borries Segovia, M.A. Estudio y Simulación de Sistemas Adaptables Fraccionarios. Ph.D. Thesis, Universidad de Chile: Santiago, Chile, May 2012.
28. Wang, Y.; Chen, J.; Yan, F.; Zhu, K.; Chen, B. Adaptive super-twisting fractional-order nonsingular terminal sliding mode control of cable-driven manipulators. *ISA Trans.* **2019**, *86*, 163–180. [[CrossRef](#)] [[PubMed](#)]
29. Rabah, K.; Ladaci, S. A Fractional Adaptive Sliding Mode Control Configuration for Synchronizing Disturbed Fractional-Order Chaotic Systems. *Circ. Syst. Signal Process.* **2019**, *39*, 1244–1264. [[CrossRef](#)]
30. Govea-Vargas, A.; Castro-Linares, R.; Duarte-Mermoud, M.; Aguila-Camacho, N.; Ceballos, G. Fractional Order Sliding Mode Control of a Class of Second Order Perturbed Nonlinear Systems: Application to the Trajectory Tracking of a Quadrotor. *Algorithms* **2018**, *11*, 168. doi:10.3390/a11110168. [[CrossRef](#)]
31. Luna, R.; López, F.; Pérez-Correa, J.R. Minimizing methanol content in experimental charentais alembic distillations. *J. Ind. Eng. Chem.* **2018**, *57*, 160–170. [[CrossRef](#)]
32. Luna, R.; Matias-Guiu, P.; López, F.; Pérez-Correa, J.R. Quality aroma improvement of Muscat wine spirits: A new approach using first-principles model-based design and multi-objective dynamic optimisation through multi-variable analysis techniques. *Food Bioprod. Process.* **2019**, *115*, 208–222. [[CrossRef](#)]
33. Brosilow, C.; Joseph, B. *Techniques of Model-Based Control*; Prentice Hall Professional: Hoboken, NJ, USA, 2002.
34. He, L.; Subramanian, V.R.; Tang, Y.J. Experimental analysis and model-based optimization of microalgae growth in photo-bioreactors using flue gas. *Biomass Bioenerg.* **2012**, *41*, 131–138. [[CrossRef](#)]
35. Vinagre, B.M.; Monje, C.A. Introducción al Control Fraccionario. *Rev. Iberoam. Autom. In.* **2009**, *3*, 5–23. doi:10.4995/riai.v3i3.8081. [[CrossRef](#)]
36. Kilbas, A.A.A.; Srivastava, H.M.; Trujillo, J.J. *Theory and Applications of Fractional Differential Equations*; Elsevier: New York, NY, USA, 2006.
37. Tepļjakov, A.; Petlenkov, E.; Belikov, J. Gain and order scheduled fractional-order PID control of fluid level in a multi-tank system. In Proceedings of the ICFDA'14 International Conference on Fractional Differentiation and Its Applications 2014, Catania, Italy, 23–25 June 2014; pp. 1–6.

38. Utkin, V.I. *Sliding Modes in Control and Optimization*; Springer Science & Business Media: Berlin, Germany, 1992.
39. Efe, M.Ö. Integral sliding mode control of a quadrotor with fractional order reaching dynamics. *Trans. Inst. Meas. Contr.* **2011**, *33*, 985–1003. [[CrossRef](#)]
40. Dewasme, L.; Coutinho, D.; Wouwer, A.V. Adaptive and robust linearizing control strategies for fed-batch cultures of microorganisms exhibiting overflow metabolism. In *Informatics in Control, Automation and Robotics*; Cetto, J.A., Ferrier, J.L., Filipe, J., Eds.; Springer: Berlin, Germany, 2011; Volume 89, pp. 283–305.



© 2020 by the authors. Licensee MDPI, Basel, Switzerland. This article is an open access article distributed under the terms and conditions of the Creative Commons Attribution (CC BY) license (<http://creativecommons.org/licenses/by/4.0/>).